J|A|C|S ARTICLES

Published on Web 07/27/2010

Direct Analysis of Donor−Acceptor Distance and Relationship to Isotope Effects and the Force Constant for Barrier Compression in Enzymatic H-Tunneling Reactions

Christopher R. Pudney,[†,‡] Linus O. Johannissen,[†,§] Michael J. Sutcliffe,[†,§] Sam Hay,[†,‡] and Nigel S. Scrutton*[,†,‡]

Manchester Interdisciplinary Biocentre, Faculty of Life Sciences, and School of Chemical Engineering and Analytical Science, University of Manchester, 131 Princess Street, Manchester, M1 7DN, United Kingdom

Received June 2, 2010; E-mail: nigel.scrutton@manchester.ac.uk

Abstract: The role of dynamical effects in enzyme catalysis is both complex and widely debated. Understanding how dynamics can influence the barrier to an enzyme catalyzed reaction requires the development of new methodologies and tools. In particular compressive dynamics—the focus of this study—may decrease both the height and width of a reaction barrier. By making targeted mutations in the active site of morphinone reductase we are able to alter the equilibrium of conformational states for the reactive complex in turn altering the donor−acceptor (D−A) distance for H-transfer. The sub-Å changes which we induce are monitored using novel spectroscopic and kinetic "rulers". This new way of detecting variation in D−A distance allows us to analyze trends between D−A distance and the force constant of a compressive dynamical mode. We find that as the D−A distance decreases, the force constant for a compressive mode increases. Further, we demonstrate that—contrary to current dogma—compression may not always cause the magnitude of the primary kinetic isotope effect to decrease.

Introduction

Enzymes catalyze a diverse array of chemical reactions, and often these reactions barely proceed in solution in the absence of the enzyme catalyst.[1] The origin of this catalytic power has no clear apparent single solution and is likely attributed to multiple factors that contribute in an enzyme specific way. This has been emphasized in studies employing a wide range of experimental[2−8] and computational[7,9−12] approaches, the interpretation of which has been debated by workers in the field.[13−17] In recent years, there has been extensive discussion about the role of dynamics in enzyme catalysis. Dynamical changes occur over different time scales ranging from domain motions (seconds) to bond vibrations (femtoseconds).[18] Owing to the complexity of dynamics inherent in enzyme systems, demonstration of dynamical contributions to mechanism and catalysis is challenging. We have studied subpicosecond vibrational modes that may cause transient compression along the reaction coordinate in hydrogen (H)-transfer reactions.[4,5,19] Often such reactions proceed via nuclear quantum mechanical (NQM) tunneling of the transferring H. For such reactions, in particular those proceeding with a large tunneling contribution, the reaction rates are dependent on both the width and height of the reaction barrier.[20] In principle, compressive modes, sometimes termed promoting modes, can decrease both barrier height and width, thereby enhancing the probability of H-transfer by either tunneling (through barrier) or classical (over-the-barrier) mechanisms.[20−22]

[†] Manchester Interdisciplinary Biocentre.
[‡] Faculty of Life Sciences.
[§] School of Chemical Engineering and Analytical Science.

(1) Lad, C.; Williams, N. H.; Wolfenden, R. *Proc. Natl. Acad. Sci. U.S.A.* **2003**, *100*, 5607.
(2) Bandaria, J. N.; Cheatum, C. M.; Kohen, A. *J. Am. Chem. Soc.* **2009**, *131*, 10151.
(3) Fraser, J. S.; Clarkson, M. W.; Degnan, S. C.; Erion, R.; Kern, D.; Alber, T. *Nature* **2009**, *462*, 669.
(4) Hay, S.; Sutcliffe, M. J.; Scrutton, N. S. *Proc. Natl. Acad. Sci. U.S.A.* **2007**, *104*, 507.
(5) Loveridge, E. J.; Tey, L. H.; Allemann, R. K. *J. Am. Chem. Soc.* **2010**, *132*, 1137.
(6) Maglia, G.; Allemann, R. K. *J. Am. Chem. Soc.* **2003**, *125*, 13372.
(7) Masgrau, L.; Roujeinikova, A.; Johannissen, L. O.; Hothi, P.; Basran, J.; Ranaghan, K. E.; Mulholland, A. J.; Sutcliffe, M. J.; Scrutton, N. S.; Leys, D. *Science* **2006**, *312*, 237.
(8) Van Vleet, J.; Kleeb, A.; Kast, P.; Hilvert, D.; Cleland, W. W. *Biochim. Biophys. Acta* **2010**, *1804*, 4.
(9) Garcia-Viloca, M.; Gao, J.; Karplus, M.; Truhlar, D. G. *Science* **2004**, *303*, 186.
(10) Saen-Oon, S.; Ghanem, M.; Schramm, V. L.; Schwartz, S. D. *Biophys. J.* **2008**, *94*, 4078.
(11) Warshel, A.; Sharma, P. K.; Kato, M.; Xiang, Y.; Liu, H. B.; Olsson, M. H. M. *Chem. Rev.* **2006**, *106*, 3210.
(12) Watney, J. B.; Hammes-Schiffer, S. *J. Phys. Chem. B* **2006**, *110*, 10130.
(13) Benkovic, S. J.; Hammes, G. G.; Hammes-Schiffer, S. *Biochemistry* **2008**, *47*, 3317.
(14) Kamerlin, S. C. L.; Warshel, A. *Proteins* **2009**, *78*, 1339.
(15) Nagel, Z. D.; Klinman, J. P. *Nat. Chem. Biol.* **2009**, *5*, 543.
(16) Papoian, G. A. *Proc. Natl. Acad. Sci. U.S.A.* **2008**, *105*, 14237.
(17) Sigala, P. A.; Kraut, D. A.; Caaveiro, J. M. M.; Pybus, B.; Ruben, E. A.; Ringe, D.; Petsko, G. A.; Herschlag, D. *J. Am. Chem. Soc.* **2008**, *130*, 13696.
(18) Yon, J. M.; Perahia, D.; Ghelis, C. *Biochimie* **1998**, *80*, 33.
(19) Pudney, C. R.; Hay, S.; Levy, C.; Pang, J. Y.; Sutcliffe, M. J.; Leys, D.; Scrutton, N. S. *J. Am. Chem. Soc.* **2009**, *131*, 17072.
(20) Hay, S.; Johannissen, L. O.; Sutcliffe, M. J.; Scrutton, N. S. *Biophys. J.* **2010**, *98*, 121.

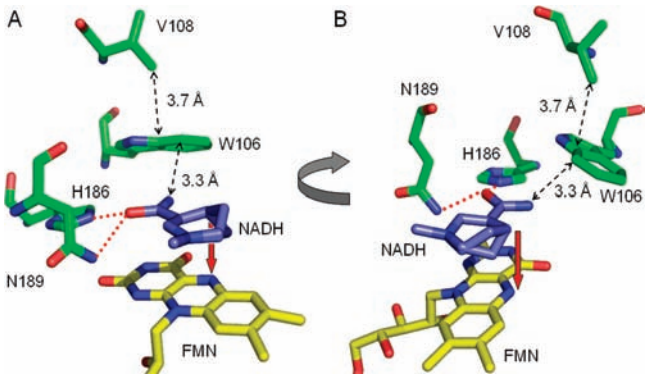

Figure 1. X-ray crystal structure[47] (2R14.pdb) of wild-type MR bound to the nonreactive NADH analogue 1,4,5,6-tetrahydroNADH$_4$ (NADH$_4$) showing key residues in the coenzyme binding site that are involved in determining the donor−acceptor (D−A) distance. Hydrogen bonds to the nicotinamide moiety are shown as red dashed lines. The direction of hydride transfer is shown as a solid red arrow. Potential compressive modes of residues V108 and W106 are shown as black dashed arrows.

The hydride transfer in the reductive half-reaction (RHR) catalyzed by morphinone reductase (MR) is well characterized.[4,23,24] A large body of experimental and computational evidence is consistent with compressive motion accompanying this reaction,[4,25,26] which involves hydride transfer from the C4 *pro-R* hydrogen of β-nicotinamide adenine dinucleotide (NADH) to the N5 atom of flavin mononucleotide (FMN) (Figure 1). This is observed directly in a rapid mixing stopped-flow instrument and is kinetically resolved from steps involving coenzyme binding and formation of an enzyme-NADH charge-transfer (CT) complex; the observed KIE is therefore the intrinsic KIE.[23] We have provided evidence from integrated kinetic, structural, and computational studies that this hydride transfer proceeds with a large contribution from nuclear quantum mechanical (NQM) tunneling.[4,24,26] The temperature-dependence of the primary kinetic isotope effect (1° KIE) has been used to infer the existence of compressive modes along the reaction coordinate in a number of enzyme systems,[2,27−30] including MR.[23] Some workers have questioned this interpretation based solely on computational studies,[14] but others have reinforced this view.[4,31,32] With MR and the related pentaerythritol tetranitrate reductase (PETNR), we have provided additional experimental data that supports the notion of rate enhancement due to compression. This has been in the form of pressure-dependence studies of 1°[4,33] and secondary (2°) KIEs[25,34] and more direct studies involving pressure-dependence analysis of the distance between nicotinamide coenzyme and FMN in the MR−NADH$_4$ complex.[4,25] These studies are consistent with the temperature-dependence of the 1° KIE in MR being sensitive to the force constant of compressive modes coincident with the reaction coordinate.[4,33] We emphasize that these studies demonstrate that the 1° KIE is dependent on both the donor−acceptor (D−A) distance and the force constant for the compressive mode(s).[33] This dual dependence is thought to account for the counterintuitive increase in KIE as the D−A distance is shortened.[4,33] Shortening of the D−A distance with pressure is also consistent with the observed increase in the hydride transfer rate with increasing pressure.[4] Such trends in experimental data can be modeled using Marcus-like frameworks for H-tunneling, adapted to incorporate changes in hydrostatic pressure.[33] Owing to their relative simplicity, these models have limitations (e.g., in determining precise D−A distances, as recognized in our previous work[4,33]) but are useful in modeling trends in the temperature and pressure dependence of kinetic data. Computational simulations are also required to visualize structural change at the atomic level, as we have done with MR[26] and other enzyme systems,[35,36] in the context of H-tunneling.

Studies with other enzymes that catalyze H-transfer reactions indicate that mutations can lead to changes in the temperature dependence of the 1° KIE.[29,37−39] It has been suggested that this reflects a change in the apparent force constant of vibrational mode(s) coupled to the reaction coordinate. Sigala et al.[17] have demonstrated the importance of microscopic, sub-Å, variation in active site orientation. Mutations, whether in the active site geometry or more distal, may induce sub-Å changes in D−A distance. These distance perturbations lead to altered functional behavior, but are too small to be analyzed (with confidence) by X-ray crystallography, especially as this requires analysis of the 'reactive' enzyme−substrate complex. Simulation studies have proved informative, particularly in uncovering networks of compressive modes;[10] however there is a need also for experimental validation. Changes in D−A distance can be modeled using phenomenological Marcus-like models,[30,40,41] but in general a more direct readout of D−A distance is required. Here we report modulation of the D−A distance for hydride transfer in MR by targeted mutagenesis of residues in the active site. We demonstrate an ability to determine directly changes in D−A distance induced by mutation. This is achieved using spectroscopic analysis of the coenzyme−FMN $\pi-\pi$ charge-transfer (CT) interaction in the enzyme−coenzyme complex coupled with detailed kinetic analysis of the α-secondary (2°) KIE. We go on to correlate D−A distance with variation in the force constant for compression along the reaction coordinate. We demonstrate how spectroscopic information can be integrated into Marcus-like models by direct measurement of the

(21) Antoniou, D.; Schwartz, S. D. *Proc. Natl. Acad. Sci. U.S.A.* **1997**, *94*, 12360.
(22) Cui, Q.; Karplus, M. *J. Am. Chem. Soc.* **2002**, *124*, 3093.
(23) Basran, J.; Harris, R. J.; Sutcliffe, M. J.; Scrutton, N. S. *J. Biol. Chem.* **2003**, *278*, 43973.
(24) Pudney, C. R.; Hay, S.; Sutcliffe, M. J.; Scrutton, N. S. *J. Am. Chem. Soc.* **2006**, *128*, 14053.
(25) Hay, S.; Pudney, C. R.; McGory, T. A.; Pang, J.; Sutcliffe, M. J.; Scrutton, N. S. *Angew. Chem., Int. Ed.* **2009**, *48*, 1452.
(26) Pang, J. Y.; Hay, S.; Scrutton, N. S.; Sutcliffe, M. J. *J. Am. Chem. Soc.* **2008**, *130*, 7092.
(27) Fan, F.; Gadda, G. *J. Am. Chem. Soc.* **2005**, *127*, 17954.
(28) Knapp, M. J.; Rickert, K.; Klinman, J. P. *J. Am. Chem. Soc.* **2002**, *124*, 3865.
(29) Kohen, A.; Cannio, R.; Bartolucci, S.; Klinman, J. P. *Nature.* **1999**, *399*, 496.
(30) Meyer, M. P.; Tomchick, D. R.; Klinman, J. P. *Proc. Natl. Acad. Sci. U.S.A.* **2008**, *105*, 1146.
(31) Mincer, J. S.; Schwartz, S. D. *J. Chem. Phys.* **2004**, *120*, 7755.
(32) Nagel, Z. D.; Klinman, J. P. *Chem. Rev.* **2006**, *106*, 3095.
(33) Hay, S.; Scrutton, N. S. *Biochemistry.* **2008**, *47*, 9880.
(34) Hay, S.; Pudney; C. R., Sutcliffe, MJ,; Scrutton, N. S. *J. Phys. Org. Chem.* In press, full text, DOI 10.1002/poc.1653.
(35) Masgrau, L.; Basran, J.; Hothi, P.; Sutcliffe, M. J.; Scrutton, N. S. *Arch. Biochem. Biophys.* **2004**, *428*, 41.
(36) Ranaghan, K. E.; Masgrau, L.; Scrutton, N. S.; Sutcliffe, M. J.; Mulholland, A. *ChemPhysChem* **2007**, *8*, 1816.
(37) Basran, J.; Sutcliffe, M. J.; Scrutton, N. S. *J. Biol. Chem.* **2001**, *276*, 24581.
(38) Quaye, O.; Gadda, G. *Arch. Biochem. Biophys.* **2009**, *489*, 10.
(39) Wang, L.; Goodey, N. M.; Benkovic, S. J.; Kohen, A. *Proc. Natl. Acad. Sci. U.S.A.* **2006**, *103*, 15753.
(40) Antoniou, D.; Schwartz, S. D. *J. Phys. Chem. B* **2001**, *105*, 5553.
(41) Johannissen, L. O.; Hay, S.; Scrutton, N. S.; Sutcliffe, M. J. *J. Phys. Chem. B* **2007**, *111*, 2631.
(42) Craig, D. H.; Moody, P. C. E.; Bruce, N. C.; Scrutton, N. S. *Biochemistry* **1998**, *37*, 7598.

D−A distance following mutation. Our work provides strong support for barrier compression in hydride tunneling in MR and (by inference) perhaps more broadly in other enzyme systems.

Materials and Methods

Enzyme and Coenzyme Preparation. All materials were obtained from Sigma-Aldrich except NAD^+ and NADH, which were from Melford Laboratories, and [$^2H_6$]-ethanol which was from Cambridge Isotope Laboratories. MR was purified as described previously.[43] The W106A, V108A, and V108L variant MR enzymes were isolated using the QuikChange mutagenesis protocol (Stratagene) and the following oligonucleotides: 5′-GCC CTG CAG CTG GCG CAC GTC GGC CG-3′ (W106A), 5′-AGC TGT GGC ACG CCG GCC GTG TCT C-3′ (V108A), and 5′-CAG CTG TGG CAC CTC GGC CGT GTC T-3′ (V108L). Plasmid pMORB3 was used as a template for the mutagenesis reactions.[43] The variant genes were completely sequenced to confirm the integrity of the construct. Expression and purification of the variant MR enzymes was as described for the wild-type enzyme.[43] (*R*)-[4-^{2}H]-NADH was prepared through stereospecific reduction of NAD^+ with [$^2H_6$]-ethanol using equine liver alcohol dehydrogenase and aldehyde dehydrogenase as described previously.[43] (*S*)-[4−2H]-NADH was prepared through stereospecific reduction of NAD^+ with [^{2}H]-glucose using glucose dehydrogenase as described previously.[43] 1,4,5,6-tetrahydroNADH ($NADH_4$) was prepared as described previously.[43] The coenzymes were purified by anion-exchange chromatography and stored freeze-dried at −80 °C. Coenzyme solutions were made fresh, and their concentrations were determined by absorbance measurements at 340 nm, $\epsilon = 6.22\ mM^{-1}\ cm^{-1}$ (NADH), or at 288 nm, $\epsilon = 16.8\ mM^{-1}\ cm^{-1}$ ($NADH_4$). Coenzyme purity was typically better than 95% determined by ^{1}H NMR (Bruker 400 MHz spectrometer, 10 mM potassium phosphate buffered D_2O, pD 7.1, 10 °C) by assessing the relative peak height of the *pro*-R and *pro*-S protons. KIE values were not corrected for this impurity.

Stopped-Flow Kinetic Studies. To prevent the oxidase activity of MR and its variant forms, all kinetic studies were performed under strict anaerobic conditions (<5 ppm O_2) within a glovebox environment (Belle Technology) as described previously.[23] An Applied Photophysics SX.18MV-R stopped-flow spectrophotometer was used for all hydride transfer studies and was wholly contained within the glovebox. Spectral changes accompanying flavin reduction were monitored at 464 nm over a log timebase (3 decades). Typically 3−5 measurements were taken for each reaction condition. For the variant enzymes, reaction transients were fit to eq 1:

$$A(t) = \sum_{i=1}^{n} A_i \exp(-k_i t)^b + A_\infty \qquad (1)$$

where $A(t)$ is the measured absorption at time t; A_∞ is the final, extrapolated absorption (to account for reactions that have not quite gone to completion); A_i is the amplitude and k_i is the rate constant of the ith exponential component, obtained from the stopped-flow trace; and b is a stretch function which describes how well each exponential component fits to a true exponential relationship. Values of $b = 1 \pm 0.2$ are considered to give an accurate fit to a single exponential component. The term b is allowed to vary only to assess the quality of fitting and is fixed to $b = 1.0$ for final extraction of kinetic data. The number of exponential components were chosen based on the number which gave $b = 1 \pm 0.2$ for the major phase and where additional exponentials did not significantly alter the extracted rate constant, k_1, of the first (fastest) kinetic phase. Individual reaction absorption traces were fit using $n = 1$ (wild-type MR); $n = 2$ (W106A); or $n = 3$ (V108A/L MR) using Origin 7 software (MicroCal). For temperature dependence studies of hydride transfer, saturating concentrations of coenzyme (5 mM for wild-type MR and V108L MR; 20 mM for W106A; 100 mM for V108A MR) were used to confer pseudo-first-order reaction kinetics. At 100 mM NADH there is a slight mixing artifact (first ∼5 ms) which was removed before fitting. Given the magnitude of k_{obs} for V108A MR, removing these points has essentially no effect on the extracted rate constant. For V108A and V108L, temperature dependence studies were over the restricted range 5−30 °C (V108A) and 10−35 °C (V108L) as the reaction transients were complex (requiring increased or decreased values of n for fitting) at lower or higher temperatures. All measurements were made in 50 mM potassium dihydrogen orthophosphate buffer, pH 7.0 containing 2 mM 2-mercaptoethanol.

Potentiometric Titrations. Redox potentiometry was performed as described previously in a Belle Technology glovebox under anaerobic conditions at 25 °C. The enzyme, typically between 40 and 50 μM, was titrated against sodium dithionite (reduction) and potassium ferricyanide (oxidation). Good electrical communication was ensured by the use of redox mediators (20 μM 2-hydroxy-1,4-napthoquinone, 8 μM phenazine methosulfate, 4 μM methyl viologen, and 4 μM benzyl viologen). Fitting to a Nernstian function describing the two electron reduction and oxidation of MR was as described previously.[19]

Numerical Modeling. Numerical modeling was based on the Kuznetsov and Ulstrup model for nonadiabatic H-transfer reactions.[44] The model and its implementation have been described previously.[20,45] The modeling is described in detail in the Supporting Information.

Molecular Dynamics Simulations. MD simulations were carried out using the CHARMM22 force field. A 10 ns unrestrained MD simulation was used to obtain the average geometries and C4−N5 distance (3.75 Å). Two 1 ns MD simulations, following 3 ns of unrestrained equilibration, were performed with the C4−N5 distance restrained to 2.65 and 3.5 Å (approximately the minimum and average distances, respectively, observed over the unrestrained equilibration step) with a force constant of 500 kcal mol^{-1} $Å^{-2}$. The effect of C4−N5 compression was estimated by comparing the average geometries (and the average geometries plus/minus one standard deviation) for these simulations and the 3−4 ns segment (i.e., the same time frame) of the unrestrained simulation.

Results and Discussion

Probing Donor−Acceptor (D−A) Distances in Wild-Type and Variant Enzymes. MD simulations of wild-type MR at various fixed D−A distances suggest that the position of the active site residues W106 and V108 are sensitive to variation in D−A distance [Supporting Information (SI) Figure S1]. These residues are close to the coenzyme nicotinamide in the enzyme−coenzyme complex. Through targeted mutagenesis, we aimed to alter the equilibrium distribution of conformational states, as we have previously reported following mutation of active site residue N189 to A189,[46,47] with consequent effect on D−A distance. We elected to remove (W106A and V108A) or increase (V108L) side chain bulk, by isolating a small series of single variants of MR with the intention of modulating the D−A distance (Figure 1). Stopped-flow studies of hydride transfer with each of the variant enzymes indicated saturation of the FMN reduction kinetics with increasing NADH concentration. Moreover, each variant enzyme forms a stable CT complex on binding $NADH_4$, displays a significant 1° KIE on the FMN reduction kinetics, and has similar midpoint reduction potentials for the enzyme−$NADH_4$ complex. These basic

(43) Hay, S.; Pudney, C. R.; Scrutton, N. S. *FEBS J.* **2009**, *276*, 3930.
(44) Kuznetsov, A. M.; Ulstrup, J. *Can. J. Chem.* **1999**, *77*, 1085.
(45) Johannissen, L. O.; Irebo, T.; Sjodin, M.; Johansson, O.; Hammarstrom, L. *J. Phys. Chem. B* **2009**, *113*, 16214.
(46) Pudney, C.; McGrory, T.; Pang, J.; Lafite, P.; Hay, S.; Sutcliffe, M. J.; Scrutton, N. S. *ChemBioChem* **2009**, *10*, 1379.

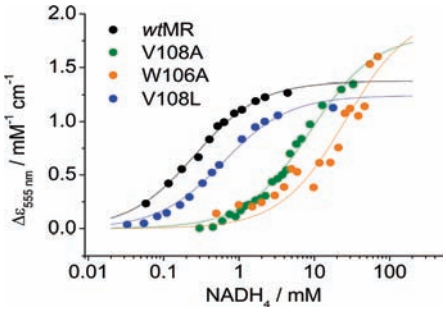

Figure 2. Titration of wild-type and variant forms of MR against $NADH_4$ showing the development of the absorbance at 555 nm of the CT complex. Wild-type, V108A, V108L, W106A. The data are fit to a weak-binding isotherm: $\varepsilon = \Delta\varepsilon[NADH_4]/(K_d + NADH_4)$. Conditions: 50 mM potassium phosphate, 2 mM 2-mercaptoethanol pH 7, 20 μM enzyme, 10 °C.

Table 1. Relative D−A Distances Determined Using CT Spectroscopy and 2° KIE Measurements

	Wild-type MR	V108L MR	V108A MR	W106A MR
CT ϵ_{max} (mM^{-1} cm^{-1})[a]	1.41 ± 0.04	1.24 ± 0.03	1.8 ± 0.05	2.3 ± 0.2
2° KIE[b]	1.18 ± 0.02[c]	1.23 ± 0.01	1.14 ± 0.02	1.13 ± 0.02
Qualitative *d*(D−A)relative to wild-type	−	Increase	Decrease	Decrease

[a] Data collected at 20 °C. [b] Data collected at 25 °C. [c] Value previously reported in *Pudney et al.*[24]

kinetic, thermodynamic and spectroscopic properties (described below) were used as probes to investigate the effects of D−A distance on kinetics, isotope effects, and the force constant for barrier compression.

It is possible to form a stable CT complex with wild-type MR and the variants studied here using the nonreactive NADH analogue, $NADH_4$.[23] This complex gives a characteristic absorbance centered at ~555 nm as a result of the $\pi-\pi$ stacking of the nicotinamide and isoalloxazine moieties. In the wild-type enzyme, this absorption increases with pressure,[25] suggesting an effective narrowing of the macroscopic reaction barrier in an ensemble of enzyme−$NADH_4$ complexes.[25,48] The absolute magnitude of CT complex absorbance therefore provides a qualitative depiction of the relative difference in the range of equilibrium D−A distances within the ensemble, effectively acting as a "spectroscopic ruler". We have now used this approach to estimate relative differences in D−A distances between wild-type and variant forms of MR (at 1 atm pressure). The dependence of the CT absorbance on $NADH_4$ concentration is shown in Figure 2, and associated parameters are given in Table 1.[49] From these data we determined the maximal extinction coefficient at 555 nm (CT ϵ_{max}). Compared to wild-type MR (CT ϵ_{max} = 1.41 ± 0.04 mM^{-1} cm^{-1}) these values indicate that there is a relative shortening of the D−A distance in V108A MR (CT ϵ_{max} = 1.8 ± 0.05 mM^{-1} cm^{-1}) and W106A MR (CT ϵ_{max} = 2.3 ± 0.2 mM^{-1} cm^{-1}) but relative lengthening in V108L MR (CT ϵ_{max} = 1.24 ± 0.03 mM^{-1} cm^{-1}).

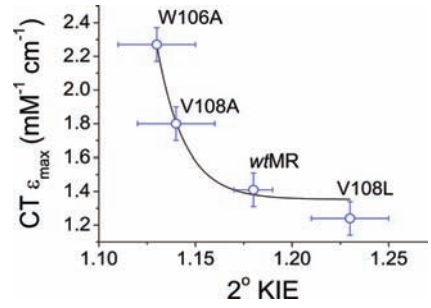

Figure 3. Correlation of the magnitude of the observed 2° KIE and absorbance maximum of the CT complex with wild-type and variant forms of MR. The black line is a fit to a single exponential decay to aid the eye. The red line illustrates the variation in D−A distance, *d*(D−A).

We emphasize that the spectroscopically accessible D−A distance is not strictly identical to that associated with H-transfer in the enzyme−NADH complex. The reactive complex is approached by thermal activation of the binary complex to a configuration at which the D−A states are degenerate, termed the tunneling ready configuration (TRC).[24] Nevertheless, the spectroscopically accessible D−A distances, and the associated changes induced by mutation, are likely to map very closely to D−A distances in the TRC. The important point is the *change* in average D−A distance, Δd(D−A), that we measure spectroscopically in the ensemble of enzyme−$NADH_4$ complexes and how this relates to parameters (kinetic isotope effects and force constants), which we analyze below.

We have suggested previously that the magnitude of the 2° KIE in MR reflects relative differences in TRC geometry,[24,50] acting as a sensitive reporter of the D−A distance at the TRC. This is supported by pressure studies of 2° KIEs, where we found that the value of the 2° KIE decreased with increasing pressure.[34] Since pressure is thought to narrow the reaction barrier, 2° KIEs can also serve as an empirical readout of barrier compression (i.e., as another "kinetic ruler"). That is, we expect the 2° KIE to decrease with shorter D−A distances. The measured 2° KIEs for FMN reduction for wild-type and variant forms of MR are given in Table 1. The 2° KIE is smaller with V108A MR (1.14 ± 0.02) and W106A MR (1.13 ± 0.02) compared to wild-type MR (1.18 ± 0.02). Conversely, the 2° KIE with V108L MR (1.23 ± 0.01) is larger than that with wild-type and the other enzyme variants. Data from the spectroscopic and kinetic rulers are therefore self-consistent in suggesting that the D−A distance is decreased in W106A/V108A MR and increased in V108L. Further, these data indicate that the differences in geometry between the reactive complexes must be small (sub-Å) as otherwise we would not observe either a measurable CT absorbance or 2° KIE. The CT and 2° KIE data are correlated in Figure 3 to illustrate the overall trend.

Probing Effects of D−A Distance on the Force Constant for Compression. We measured the observed rate constant of FMN reduction by NADH and (*R*)-[4-^{2}H]-NADH in each of the variant enzymes. Stopped-flow transients for each of the variant enzymes (SI Figure S2) are multiexponential, consistent with an expansion of the accessible energy landscape in the enzyme−coenzyme complex.[46,47] Such an expansion has been characterized in detail in an N189A variant which gave rise to the concept of multiple reactive configurations (MRCs) and

(47) Pudney, C. R.; Hay, S.; Pang, J. Y.; Costello, C.; Leys, D.; Sutcliffe, M. J.; Scrutton, N. S. *J. Am. Chem. Soc.* **2007**, *129*, 13949.
(48) Ewald, A. H.; Scudder, J. A. *J. Phys. Chem.* **1972**, *76*, 249.
(49) We would like to apply this type of analysis to the previously characterized N189A MR variant. However, it appears that N189 provides important restraint to the nicotinamide, making analysis of the contributions to CT complex absorbance difficult due to the vast increase in conformational heterogeneity.[46] We are presently developing methodologies to dissect systems which have such greatly expanded free energy landscapes for the reactive complex.

(50) Hay, S.; Pang, J. Y.; Monaghan, P. J.; Wang, X.; Evans, R. M.; Sutcliffe, M. J.; Allemann, R. K.; Scrutton, N. S. *ChemPhysChem* **2008**, *9*, 1536.

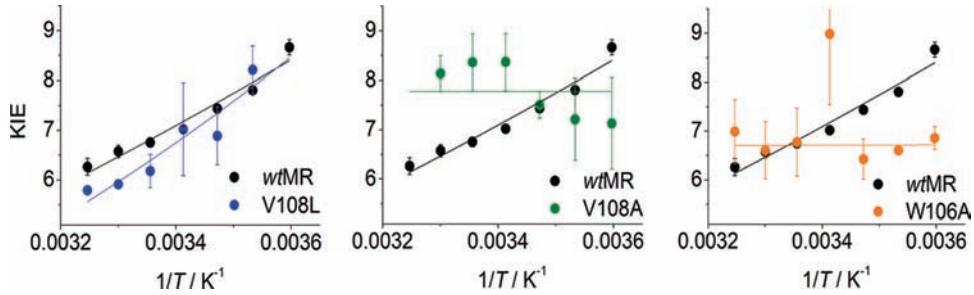

Figure 4. Temperature-dependence of the 1° KIE with (A) V108L, (B) V108A and (C) W106A MR compared to wild-type MR (black). Solid lines show fits to a modified version of eq 2 reported in ref 33. Conditions: 50 mM potassium phosphate; pH 7; 2 mM 2-mercaptoethanol; 20 μM enzyme; and 5 mM (V108L MR), 100 mM (V108A MR), or 20 mM (W106A MR) NADH.

Table 2. Parameters Determined from Temperature Dependence Studies of Flavin Reduction and Redox Potentiometry

	Wild-type MR	V108L MR	V108A MR	W106A MR
k_{obs} (s^{-1})[a]	56.4 ± 0.77[b]	44.5 ± 0.2	32.9 ± 0.9	36.1 ± 2.5
1° KIE[a]	6.8 ± 0.1	6.2 ± 0.3	8.4 ± 0.6	6.8 ± 0.7
$\Delta H^{\ddagger}$ (kJ mol^{-1})	35.8 ± 0.6[b]	31.0 ± 0.4	48.2 ± 2.5	43. ± 3.5
$\Delta\Delta H^{\ddagger}$ (kJ mol^{-1})	7.4 ± 1.5	10.9 ± 1.7	−1.9 ± 4.3	1.7 ± 5.6
E_m (mV)[a]	−258 ± 2	−264 ± 2	−219 ± 1	−

[a] Data collected at 25 °C. [b] Data reported in *Pudney et al.*[24]

parallel pathways for hydride transfer in MR.[47] For the variant enzymes reported here, the additional phases observed in stopped-flow studies are required only for accurate fitting of the first phase. This is the major kinetic phase (>∼75% of the total amplitude), and rate constants extracted from this phase show saturation behavior as a function of coenzyme concentration (SI Figure 3). The 1° KIEs for this phase at saturation are >2 and there is a linear temperature dependence on the rate constant obtained from data fitting suggesting this phase is accurately reporting on FMN reduction. More information on the fitting criteria is given in *Materials and Methods*.

The temperature dependence of the observed rate constant of FMN reduction and the 1° KIEs for wild-type and variant enzymes are shown in Figure 4. The magnitude of the 1° KIEs are broadly similar for the wild-type and variant forms of MR (∼7 at 25 °C; Table 2). The resulting parameters obtained from these temperature dependence studies are given in Table 2. We remeasured the temperature dependence of the 1° KIE with wild-type MR as previously there was a reported small amount of isotopic impurity (∼9%)[24] and we recently demonstrated that this level of impurity can lead to errors in determining temperature dependence parameters.[51] The temperature dependence measured here ($\Delta\Delta H^{\ddagger}$ = 7.4 ± 1.5 kJ mol^{-1}) is similar to that published previously ($\Delta\Delta H^{\ddagger}$ = 8.9 ± 1.5 kJ mol^{-1}).[24] For the W106A and V108A variants of MR, the temperature dependence of the 1° KIE is diminished ($\Delta\Delta H^{\ddagger}$ = −1.9 ± 4.3 kJ mol^{-1} for V108A MR and 1.7 ± 5.6 kJ $mol^{-1}$for W106A MR). In comparison, the temperature dependence of the 1° KIE for V108L MR ($\Delta\Delta H^{\ddagger}$ = 10.9 ± 1.7 kJ mol^{-1}) is increased over that for wild-type MR.

One can model the KIE and $\Delta\Delta H^{\ddagger}$ values using a modified Marcus-like model that incorporates a function to account for compressive motion. Numerical modeling using Meyer and Klinman's modification of the Kuznetsov and Ulstrup nonadiabatic model for H-tunneling (eq 2)[52] gives values for the

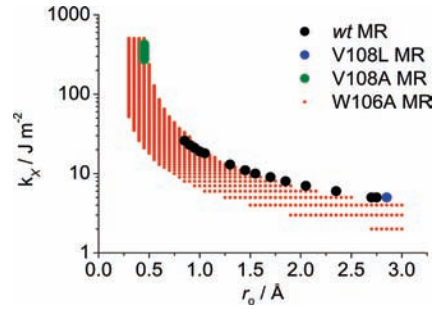

Figure 5. Modeling of the r_0 and promoting vibration force constant dependence of the KIE using the Kuznetsov and Ulstrup vibronic model with the H wave function modeled using a Morse potential as described previously.[20] Solutions to eq 2 are shown for wild-type MR, V108L MR, V108A MR, and W106A MR.

equilibrium tunneling distance, r_0, and the force constant for the compressive mode, k_X.

$$k_{CEP} = \sum_{\mu} P_{\mu} \sum_{\nu} \frac{1}{2\pi} \left| V_{EL} \right|^2 \sqrt{\frac{4\pi^3}{\lambda k_B T \hbar^2}} \exp\left\{ \frac{-\Delta G^{\ddagger}_{\mu\nu}}{k_B T} \right\} \times \left(\int_{\Delta r=0}^{\infty} \left[\left\langle \varphi_{\mu} \middle| \varphi_{\nu} \right\rangle_{\Delta r} \frac{\exp(-E_X/k_B T)}{\int_{\Delta r=0}^{\infty} \exp(-E_X/k_B T) dr} \right] dr \right)^2 \quad (2)$$

Specific details of the model and its implementation are given in the Supporting Information. We do not extract specific values for these parameters, but rather a series of values for r_0 [the equilibrium d(D−A)] and k_X [the force constant of a harmonic oscillator that describes the apparent compressive mode(s)] which satisfy eq S1. Figure 5 shows those values of r_0 and k_X where the calculated KIE and $\Delta\Delta H^{\ddagger}$ values agree with the experimental KIE ($\pm 3\ \sigma$) and $\Delta\Delta H^{\ddagger}$ ($\pm 1\ \sigma$) values (given in Table 2) for wild-type MR, V108L MR, V108A MR, and W106A MR. The KIE and $\Delta\Delta H^{\ddagger}$ values in Figure 5 were calculated with a resolution of k_X and r_0 values of 1 J m^{-2} and 0.05 Å, respectively, resulting in the 'pixelation' of the figure, and the actual solutions would be expected to form smooth and continuous regions encompassing the plotted points. The range in calculated r_0 and k_X values for each enzyme is given in Table 3. This modeling should only be treated qualitatively, and we will only use it to consider trends across the series of MR enzymes we have studied. Examination of Figure 5 shows that r_0 is shorter in V108A MR (r_0 = 0.45 Å) and longer in V108L MR (r_0 = 2.85 Å) relative to wild-type MR (r_0 = 0.85−2.75 Å). The large region of W106A values arises due to the greater experimental error in $\Delta\Delta H^{\ddagger}$, which increased the potential overlap in r_0/k_X space. While there is a large spread of W106A

(51) Hay, S.; Pudney, C. R.; Hothi, P.; Scrutton, N. S. *J. Phys. Chem. A* **2008**, *112*, 13109.
(52) Meyer, M. P.; Klinman, J. P. *Chem. Phys.* **2005**, *319*, 283.

Table 3. Parameters Determined from Numerical Analysis Using the Kuznetsov and Ulstrup Model

	Wild-type MR	V108L MR	V108A MR	W106A MR
r_0 (Å)	0.85−2.75	2.85	0.45	<0.55[a]
k_X (J m^{-2})	5−26	5	272−426	>50[a]
Qualitative Δr_0	−	Increase	Decrease	Decrease
Qualitative Δk_0	−	Decrease	Increase	Increase

[a] Data represent ~80% of solutions to the model (eq 2 and Figure 5).

MR values (r_0 = 0.3−3 Å), 80% of the calculated r_0 values fall below 0.55 Å (Table 3), suggesting that r_0 is also likely to be shorter in W106A MR than in wild-type MR. Similar trends are observed if we consider the apparent force constant of the compressive motion. The calculated k_X values are significantly larger in V108A MR (k_X = 272−426 J m^{-2}) than in wild-type MR (k_X = 5−26 J m^{-2}). The only k_X value that reproduces the experimentally determined KIE and $\Delta\Delta H^{\ddagger}$ values for V108L MR (k_X = 5 J m^{-2}) overlaps with the lower region of wild-type MR values (Table 3), suggesting that the force constant may be lower in this mutant than in wild-type MR. A large spread in values is again found for W106A MR (k_X = 2−505 J m^{-2}), but k_X > 50 J m^{-2} in 80% of the calculated cases of overlap, suggesting that the force constants are likely to be larger in W106A MR than in wild-type MR. We have previously used the pressure-dependence of the 1° KIE as an additional probe of k_X.[4] However, high pressure has been shown to alter the equilibrium of conformational states in an MR variant enzyme.[46] Such an effect complicates the analysis significantly, and as such we do not include a pressure-dependence study in the present article.

The observed trend for the change in tunneling distance, derived from numerical modeling of the temperature-dependence data, mirrors the observed trend for the D−A distance from our spectroscopic and kinetic "rulers". Moreover, as the D−A distance/r_0 decreases, the force constant of the compressive mode appears to increase. That is, the vibration effectively becomes "harder" (frequency increases) at shorter transfer distances and "softer" at larger transfer distances.

In an earlier study, Meyer et al. demonstrated that an increase in the bulk of an active site residue in soybean lipoxygenase-1 (SLO-1) was correlated with a decrease in the temperature-dependence of the 1° KIE.[30] Numerical modeling using a similar approach to eq 2 then suggested that the effect of the mutations was to decrease the D−A distance as the bulk of the residues increased. For the majority of cases, modeling the temperature-dependence of the 1° KIE using eq 2 will yield, with decreasing r_0 (and thus the D−A distance), a decreasing temperature-dependence of the 1° KIE. In the present study we have been able to monitor the change in D−A distance experimentally. Contrary to the study of Meyer et al.,[30] we find an increase in D−A distance as active site residue bulk increases. Clearly the relationship between side chain bulk and D−A distance may be complex and sometimes at odds with the (simplistic) concept that greater side chain bulk leads directly to a shorter D−A distance. As we have demonstrated previously with MR, the equilibrium of conformational states for the reactive complex can be shifted significantly upon mutation. The equilibrium of conformational states will be determined by physicochemical properties which vary in a residue/enzyme specific manner. It is for this reason that we stress the importance of establishing the effect of mutation on D−A distance by experiment or simulation (where possible) rather than relying on numerical modeling alone. That said the present study correlates well with the results of numerical modeling using eq 2.

The 1° KIE is Affected by Both D−A Distance and k_X. Kamerlin and Warshel[53] have recently discussed a large body of our work relating to the occurrence of compressive modes, particularly in MR.[4,19,25,26,33] Their discussion exposes a misunderstanding of our experimental work and conclusions. We will comment here on the most substantive point from this article (a more detailed appraisal will be presented elsewhere). Kamerlin and Warshel have argued (correctly) that, in the absence of additional factors, the magnitude of the 1° KIE will fall as the D−A distance decreases.[53] However, our pressure-dependence study of MR[4,33]—and contrary to the claim made in ref 53—demonstrates explicitly that an increase in k_X can lead to an increase in the magnitude of the 1° KIE even as the D−A distance is reduced. This was achieved through numerical modeling using the Marcus-like framework used in the current work (eq 2). We emphasize that our modeling of temperature/pressure-dependent isotope effects and rates of H-transfer is consistent with, and not proof of, Marcus-like models for H-transfer. In the present study, the magnitude of the 1° KIE remains large and varies little with changes in D−A distance (Table 2). This suggests there is opposition of a decreasing 1° KIE due to decreasing D−A distance but an increase in the 1° KIE caused by the increase in k_X. The effect is to keep the magnitude of the 1° KIE approximately constant. These experimental findings are consistent with our previous work and demonstrate that the 1° KIE need not always decrease with decreasing D−A distance. This provides further evidence[4,19,23−26,33] to support the involvement of a compressive mode along the reaction coordinate for the MR−NADH complex. The inference is that there is no 'problematic relationship between the KIE and barrier compression' as claimed by Kamerlin and Warshel.[53] The simple picture presented by Kamerlin and Warshel does not recognize variation in the frequency of putative promoting modes and does, therefore, not account for more complex relationships—resulting from dynamical effects—for the magnitude of the KIE as a function of compression. Given the consistent body of kinetic and spectroscopic data we and others have accumulated, and in the absence of convincing alternative explanations, we feel models which incorporate at least the potential for compression—whether it be to reduce the tunnelling distance or to lower the free energy barrier—are reasonable representations with which to model experimental data.

Is it Appropriate to Correlate k_{obs} with k_X? There is a persisting notion that vibrational modes that transiently cause compression along the reaction coordinate may enhance the rate of a chemical reaction,[10] particularly for H-transfers.[4,7,25,27,30,54] Compression may decrease both the width and height of the reaction barrier.[20,55,56] Decreasing the height enhances the probability of forming a transition state, and decreasing the width (effectively the D−A distance) enhances the probability of NQM tunneling. Simulation studies have suggested that the NQM contribution to the rate may decrease as barrier width decreases, since formation of the transition state becomes more favored.[20,55] However, this does not mean that the probability of tunneling

(53) Kamerlin, S. C. L.; Warshel, A. *FEBS Lett.* **2010**, *584*, 2759.
(54) Agrawal, N.; Hong, B. Y.; Mihai, C.; Kohen, A. *Biochemistry* **2004**, *43*, 1998.
(55) Olsson, M. H. M.; Parson, W. W.; Warshel, A. *Chem. Rev.* **2006**, *106*, 1737.
(56) Johannissen, L. O.; Scrutton, N. S.; Sutcliffe, M. J. *J. R. Soc. Interface* **2008**, *5*, S225–S232.

is decreased (it will in fact be enhanced), but rather that the amount of tunneling, relative to over-the-barrier transfers, is decreased. Clearly this effect will be more or less important depending on the degree of barrier compression and the individual characteristics of any given reaction barrier, particularly the width. Recent experimental evidence from a unmodified enzyme system suggests that compression can give a modest rate enhancement.[19] Whether this contribution comes primarily from over-the-barrier or through-the-barrier transfer or some combination of both is as yet unknown.

In the present study we observed an apparently large variation in k_X and D−A distance. At the same time k_{obs} varies little between each of the variant and wild-type MR enzymes with an average rate and standard deviation of $42.5 \pm 10.5\ s^{-1}$. The expected decrease in k_{obs} as D−A distance increases[20] is therefore not observed. Variation in driving force, $\Delta G°$, may account for the approximately constant k_{obs} values, effectively offsetting the decrease in k_{obs} caused by a change in D−A distance. We have measured the midpoint reduction potentials of the FMN in wild-type and V108A/L variant enzymes in complex with $NADH_4$ (SI Figure 4). With V108A, we find that E_m (Table 2) is ∼40 mV more positive than that with wild-type MR, whereas the E_m for V108L is similar to that for the wild-type enzyme. An offset of k_{obs} therefore cannot be explained by a change in $\Delta G°$ as this would require V108A MR to have a smaller value of $\Delta G°$ than the wild-type enzyme. We have not measured the E_m for W106A as the large dissociation constant for the W106A−$NADH_4$ complex (SI Figure 3) makes analysis difficult. We suggest that a plausible explanation for the invariant k_{obs} values is due to the softening (decreasing k_X) of some compressive mode as the D−A distance increases. In other words, compression provides a rate enhancement that offsets the negative effects of increasing D−A distance.

Clearly the contributions to k_{obs} are numerous and complex (see eq 2) and not all parameters can be accurately quantified by experiment or simulation. As such, it is our view that while the present data could be used as evidence that compression affords a rate enhancement in MR, attempts to correlate k_{obs} and k_X for H-transfers in mutant/enzyme variant studies might be difficult to justify. Of course the converse is also true in that we cannot rule out a rate enhancement due to a compressive mode, particularly given the weight of evidence presented in the present study. Indeed, we have recently reported data suggesting that compressive modes can provide a small rate enhancement in the related flavoprotein PETNR.[19] In this case the comparison was between two near identical substrates (NADH and NADPH) in a unmodified (wild-type) enzyme system, with little variation in D−A distance.

Conclusions

We have made targeted mutations to an enzyme active site, modulating the D−A distance. This is achieved by altering the free energy landscape for the reactive complex, perturbing it to new D−A configurations not accessible in the wild-type enzyme. We are able to monitor this sub-Å variation in D−A distance experimentally by combining evidence from both static absorbance measurements and KIE analysis. The qualitative variation in D−A distance from our experimental "rulers" is consistent with our independent numerical modeling based on a temperature-dependence analysis. We find that as the D−A distance decreases, the force constant for a compressive mode appears to increase. This opposing relationship is proposed to be the source of the near invariance of the observed 1° KIE despite the apparent variation in D−A distance. There is a tendency to assume that a decrease in D−A distance/r_0 will cause a decrease in the magnitude of the 1° KIE. However, the numerical modeling in the present study demonstrates that while a decrease in D−A distance lowers the 1° KIE, an increase in force constant of a compressive mode coupled to the reaction coordinate has the opposite effect. Combined with evidence from our previous pressure-dependence studies we believe this finding should act as a warning to those attempting to infer D−A variation based on the magnitude of the 1° KIE alone, particularly as compressive modes may be a feature of both solution and enzyme catalysis.

Acknowledgment. This work was funded by the UK Biotechnology and Biological Sciences Research Council (BBSRC). S.H. is a BBSRC David Phillips Research Fellow. N.S.S. is a BBSRC Professorial Research Fellow and Royal Society Wolfson Merit Award Holder.

Supporting Information Available: MD simulations at various D−A distances, example stopped-flow transients, concentration dependences of k_{obs} with NADH and redox titrations with $NADH_4$ bound for wild-type and variant enzymes. and details of numerical modeling. This material is available free of charge via the Internet at http://pubs.acs.org.

JA1048048